DTIC FILE COPY

AD-A202 593

DTIC
ELECTE
JAN 1 8 1989
S D
CD

DISTRIBUTION STATEMENT A
Approved for public release;
Distribution Unlimited

DEPARTMENT OF THE AIR FORCE

AIR UNIVERSITY

AIR FORCE INSTITUTE OF TECHNOLOGY

Wright-Patterson Air Force Base, Ohio

89 1 17 045

(1)

AFIT/GEO/ENP/88D-3

DTIC
ELECTE
JAN 1 8 1989
S D
D CS

EVALUATION OF THE SPATIAL AND TEMPORAL CHARACTERISTICS OF THE CONDUCTING PRIZ

THESIS

Patrick J. Gardner
Captain, USAF

AFIT/GEO/ENP/88D-3

Approved for public release; distribution unlimited

AFIT/GEO/ENP/88D-3

EVALUATION OF THE SPATIAL AND TEMPORAL CHARACTERISTICS OF THE CONDUCTING PRIZ

THESIS

Presented to the Faculty of the School of Engineering

of the Air Force Institute of Technology

Air University

In Partial Fulfillment of the

Requirements for the Degree of

Master of Science in Electrical Engineering

DTIC COPY INSPECTED 6

Accesion For
NTIS
DTIC
Unannounced
Justification
By
Distribution
Availability Codes
Dist
A-1

Patrick J. Gardner, B.S.

Captain, USAF

December 1988

Approved for public release; distribution unlimited

Preface

This thesis is a continuation of research efforts at AFIT on the conducting PRIZ. Surface layer damage in the conducting PRIZ results in degraded performance. This surface damage is introduced during grinding and polishing of the crystal; therefore, we obtained several crystals which were more carefully prepared to reduce such damage. One goal of this thesis was to re-evaluate the performance of the conducting PRIZ with these new crystals. In addition, I was interested in quantifying the spatial resolution of the device and evaluating the curious spatial-temporal characteristics of the modulator which produce dynamic imaging. These characteristics have not been reported previously on devices made outside the Soviet Union, and reports on Soviet devices are incomplete.

I am grateful to Dr. Theodore Luke, my thesis advisor, for his patience and enthusiasm throughout the thesis quarters. He was always available to discuss results and share his expertise, yet he allowed me the freedom to design and direct my research independently. I want to thank my wife Katerina who, without a doubt, has had the toughest job for the last 18 months in sustaining our family through her unending love and support. I also thank my lovely children: Emily, Erin, Mary, Kevin, and Curtis ("C.J.") who continually fill me with joy. They make this whole endeavor worthwhile.

Patrick J. Gardner

Table of Contents

List of Figures

List of Tables

Abstract

The imaging properties of the conducting PRIZ were re-evaluated using crystals which were carefully ground and polished to minimize surface layer damage. Resolution was quantified as a function of the energy density of the write-beam for both incoherent and coherent light sources. Maximum resolution from a standardized bar chart was determined using a model derived from a hybrid of luminance ratios used to evaluate image quality and the Rayleigh criteria for two point resolution. In addition, the spatial-temporal frequency dependence of the conducting PRIZ in the dynamic imaging mode was demonstrated and, for the the first time, quantified for coherent illumination over a range of spatial and temporal frequencies. Finally, the write-beam-induced damage threshold for these "carefully prepared" crystals was determined in terms of energy density.

For an incoherent write-beam with light in the 360-510 nm range, the maximum measured resolution was found to peak at 20 lp/mm and 25 $\mu J/cm^2$. Additional energy on the device did not improve the output resolution. Coherent illumination with a HeCd laser at 442 nm produced peak resolution of 40 lp/mm at 90 $\mu J/cm^2$. Optical memory of the device was found to last for 20-60 minutes, depending on the specific spatial frequency, at these peak energy densities when a single pulse of write-beam was applied. When multiple pulses of write-beam energy were applied, the frequency of the pulses (temporal frequency) as well as the energy density of the beam and spatial frequency of the object

influenced memory decay. These memory characteristics have direct implications on using the conducting PRIZ as a moving target indicator.

Catastrophic damage was found to occur for write-beam energy densities of 1150-1430 $\mu J/cm^2$ at low spatial frequencies and at higher energy densities for higher spatial frequencies. This is only slightly higher than that reported in previous AFIT research, although spatial frequency of an input image had not been previously considered a variable.

EVALUATION OF THE SPATIAL AND TEMPORAL CHARACTERISTICS OF THE CONDUCTING PRIZ

I. Introduction

Optical signal processors, which take advantage of the inherent speed and parallel nature of light in performing two-dimensional, high-speed processing of information, are crucial to the success of next generation target recognition systems. The processors require a device which can transmit a spatially modulated optical signal in real time. One device that falls in this large category of spatial light modulators that has been predicted to operate at ten times current television frame rates is the PRIZ light modulator (6:3847). PRIZ is a Soviet acronym (Preobrasovatel Izobrazheniya) that simply translates as image transformer (6:3846). The PRIZ uses a thin [110] or [111] cut of a bismuth silicon oxide (BSO) crystal. Unlike the more familiar Pockels Readout Optical Modulator (PROM), which is a [100] cut BSO crystal and modulates light via the longitudinal electro-optic effect, the PRIZ utilizes the transverse electro-optic effect which results in a superior diffraction efficiency and resolution over the standard PROM devices (4:3849).

One particularly interesting version of the PRIZ has semi-transparent electrodes which have been evaporated directly on the opposite surfaces of the crystal with a fixed voltage applied to these electrodes. This configuration is referred to as the "conducting" PRIZ (21:1) and appears promising for many high-speed image processing

applications in that the conducting PRIZ may be operated in any of the imaging modes of the standard PRIZ (12:385) as well as in a dynamic image selection mode. In this mode, only changes in an input image are transmitted while stationary objects are suppressed. Figure 1 shows a typical conducting PRIZ with its crystallographic orientations labeled.

The only known successful fabrication and operation of the conducting PRIZ outside the Soviet Union has been at the Air Force Institute of Technology (AFIT) at Wright-Patterson Air Force Base, Ohio and is reported in references 11 and 20.

Operating the PRIZ in imaging applications which require relatively high write-beam energies results in a light-induced degradation of the crystal surface. This "laser-induced damage" was first reported and

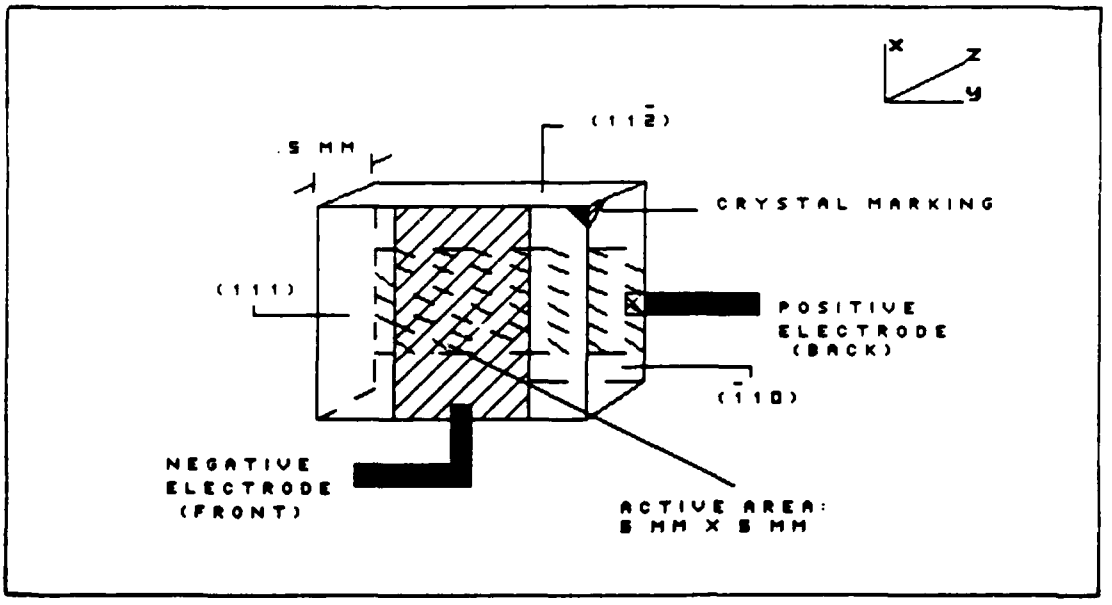

Figure 1. Typical Conducting PRIZ.

evaluated in detail by Anderson (1:4.15). Anderson indicates that the extent of crystal damage is related to surface disorders caused by mechanical preparation (grinding and polishing) of the material (1:1.2). These surface disorders and the resultant damage threshold of the PRIZ place limitations on the total write-beam energy which may be applied to the device. Anderson suggested that the energy density required for the dynamic imaging mode of the conducting PRIZ may be in the range of the damage threshold.

For this thesis, several "carefully prepared" BSO crystals were obtained from Sumitomo Electric Industries and evaluated for general imaging characteristics. This report contains spatial resolution data of the conducting PRIZ for various energy densities of both coherent and incoherent write-beam sources. Coherent resolution has only been reported on Soviet-made devices, and the PRIZ type ("standard" or "conducting") is not specified. Resolution from incoherent sources has not been previously reported. The relationship between spatial and temporal frequencies of the recording image is then evaluated and quantified for a specific energy density. This spatial-temporal dependence has only been alluded to previously in the literature. The results here are reported in a form which allows comparison with data reported in the Soviet literature on similar Soviet-made devices. Finally, the damage levels of these new crystals are reported based on damage observed during testing.

II. Background

BSO is a photoconductive material and is optically isotropic, belonging to the 23 cubic symmetry point group. In addition, BSO is optically active. The theory of operation of BSO in the PRIZ configuration ("standard" or "conducting") is nicely summarized by Anderson (1:2.2-2.3):

> The device works on the principle of photorefraction, i.e. light induced changes in the refractive indices via the transverse electro-optic effect. A longitudinal field is established by the application of a d.c. voltage between the electrodes, with the negative electrode on the "front", or illuminated, surface. The crystal is then illuminated from the front with a write-beam of suitable wavelength (not necessarily coherent). Donors are excited from deep donor centers and drift, under the influence of the applied E-field, until they are trapped at trap centers. Donor centers have been identified as silicon vacancies, and the trap centers as luminescence centers. The donors may, at this point, be thermally detrapped or optically re-excited and drift to another trap center. Thermal detrapping is a very slow process. The resulting space-charge field spatially modulates the refractive indices in the illuminated region of the crystal, via the electro-optic effect. The induced birefringence, in turn, affects the polarization of light passing through that region.
>
> When the crystal is illuminated from the front with a coherent second beam, the modulated indices are "read". This read-beam must be of wavelength such that excitation of donors due to this beam is minimal. The PRIZ is located between two polarizers which, after accounting for the optical activity of the crystal itself, are effectively crossed. Thus, the read-beam will not pass the second polarizer, or analyzer, except where the index of refraction in the crystal has been modulated by the write-beam, causing the polarization to change. The amplitude of the coherent read-beam, after passing the crossed polarizers, is related to the intensity of the original input image.

The photorefractive index change depends on the relative intensity of the incident beam rather than the total intensity, and a beam of small intensity at the correct wavelength can produce a significant electrostatic field by interacting with the BSO material for a long enough time. Thus, the magnitude of the photorefractive index change

depends on the optical energy rather than the optical intensity of the write-beam (7:418). The transverse write-induced fields within the crystal may be erased by uniformly illuminating the crystal surface with light of suitable wavelength (typically from the write-beam source).

Very little published data on the PRIZ outside of the Soviet Union are available. Casasent et al evaluated five PROM and PRIZ units which were fabricated at the A.F. Ioffe Physico-Technical Institute (FTI) in the U.S.S.R. (6:3846), and report experimental confirmation of three input image processing applications of the PRIZ: automatic suppression of low spatial frequencies (this spatial filtering characteristic creates edge-enhanced output images which are desirable for real-time correlation algorithms), directional filtering (edges are suppressed in a specific direction as a function of the polarization state of the reading beam), and dynamic image selection (which requires the conducting PRIZ version).

The performance characteristics of the PRIZ units which were fabricated at FTI and evaluated by Casasent et al are summarized in Table 1. Two caveats to this table are necessary. First, Casasent makes no clear distinction between the "standard" and "conducting" versions of the device in the reported performance specifications. Second, the data is derived from a combination of actual measurements plus data which was reported by FTI in Soviet literature (6:3848). Thus, while the three image processing applications of the Soviet-made PRIZ were demonstrated, many of the actual performance specifications were not experimentally verified.

The storage capabilities of the conducting PRIZ which was fabricated at AFIT are reported in reference 11. Maximum optical memory

Table 1.

Soviet PRIZ Performance Characteristics (5:3848)

Write-beam	Wavelength	350-500 nm
	Exposure (typical)	50 $\mu J/cm^2$
Read-beam	Wavelength	633 nm
	Power density (typical)	2 mW/cm^2
Write time	Minimum	7 nsec
	Output visible	1 μsec
	Output maximum	10 μsec
Erase time	Minimum	2 msec
Write-read-erase cycle time	Minimum	2.01 msec
Frame rate	Demonstrated	20 frames/sec
	Predicted	500 frames/sec
Storage times (typical exposure)	Dark storage	1 min
	With read-beam on	20-30 sec
Dynamic imaging	Scan rate for peak optical output	7 mm/sec
	Background suppression (maximum)	50/1

is achieved with write-beam energy densities of 25-45 $\mu J/cm^2$, while dynamic imaging is reported to require greater than 50 $\mu J/cm^2$ (11:19). The damage threshold level of these devices has been determined to be 100-200 $\mu W/cm^2$, and higher threshold levels have been predicted for crystals with reduced surface disorders (2:80).

One interesting trend is apparent in all of the reported experiments performed on the PRIZ devices. The write-beam does not need to be a coherent source. Any source with sufficient energy to induce a space-charge field in the crystal may be used (11:9). Yet every reported experiment has used either an Argon ion laser (6:3853, 20:24) or a HeCd laser (11:13, 1:4.4). As Goodman points out, the Coherent Transfer Function (CTF) and the Optical Transfer Function (OTF - systems which use incoherent illumination) cannot be directly compared (9:127) as the former is in terms of complex field amplitudes, and the latter is in terms of field intensities, but the fundamental differences between the two types of illumination in imaging systems may be summarized as follows (8:507-513, 9:125-133):

1. The maximum frequency component (cutoff frequency) of the image intensity of the OTF is twice that of the image amplitude of the CTF for a diffraction-limited system.
2. The CTF has a sharp discontinuity at its cutoff frequency which results in a characteristic "ringing" of an image. This ringing is absent in the OTF which has a gradual rolloff across its frequency band.
3. Coherent illumination is sensitive to even small optical imperfections (such as dust or small scratches) which may create pronounced diffraction patterns that will be superimposed on the image.
4. Aberrations in the imaging system affect only the phase of Fourier components within the passband of the CTF, while both the amplitude and phase of the OTF are affected. The

implication here is that incoherent imaging is more degraded by aberrations.

The above summary implies that using an incoherent write-beam of an appropriate wavelength range (350-500 nm) for imaging an object on the surface of the PRIZ may deserve closer attention, especially where aberrations are not predominant.

The only additional data on the PRIZ performance characteristics are reported in the Soviet literature, and reference to the "standard" versus "conducting" versions is often indistinguishable. In addition, Soviet literature has alluded to an interaction between spatial and temporal frequency (time-varying write-beam image obtained by on/off switching, intensity variation over time, or a nonstationary portion of the image) which controls the dynamic imaging mode in the PRIZ. For dynamic imaging, which requires the conducting version, Petrov reports that as the spatial frequency of an object increases, the peak output of the crystal for that object shifts to a lower temporal frequency (15:165). In the case of a moving object, temporal frequency is directly related to velocity. This spatial-temporal influence is not quantified in the Soviet literature and only briefly addressed in one article outside the Soviet Union (6:3852).

III. Problem Statement

The imaging properties of the conducting PRIZ needed to be thoroughly re-evaluated using BSO crystals which had been more "carefully prepared" to allow the use of higher energy density write-beams (1:7.3). Specifically, the crystals had to be evaluated for general image quality improvement with a primary focus on the more practical aspects of using the conducting PRIZ for image processing applications. In addition, information on the spatial and temporal characteristics of the conducting PRIZ in the dynamic imaging mode was inadequate. Therefore, the imaging characteristics of the device needed to be quantified over a broad range of write-beam energy densities, spatial and temporal frequencies, as well as read-beam intensity and polarization.

Scope

The scope of this research was limited to an evaluation of the "carefully prepared" BSO crystals configured in the conducting PRIZ version. While all three of the imaging features of the device were demonstrated (suppression of low spatial frequencies, directional filtering, and dynamic image selection) to verify operation of the new crystals, quantitative analysis was limited to the influence of spatial frequency, temporal frequency, and write-beam energy density on the PRIZ. Therefore, certain phenomena which were observed during the research are reported for completeness but are not quantified. Throughout this research, the device was considered for feasibility in two specific imaging applications: real-time optical correlation where the edge-enhanced image at the output of the conducting PRIZ may be

optimized based on resolution data, and a moving target indicator where dynamic imaging may be optimized as a function of the resolution data as well as write-beam energy density and temporal changes in the image.

Approach

The research was divided into three distinct stages. First an incoherent write-beam source (pressure broadened mercury lamp with a 360-510 nm filter) was used to obtain data from a standardized resolution test chart. Resolution was computed using a Rayleigh-type criteria which is described in Chapter IV. These tests involved low intensity beams (less than 5 $\mu W/cm^2$) with variable recording times. In addition, optical memory of the conducting PRIZ was re-evaluated with spatial and temporal frequency of the input image considered as variable parameters.

The second stage involved similar measurements except a coherent write-beam source was used (HeCd laser at 442 nm). In this series, the intensity was varied from 5 to 15,000 $\mu W/cm^2$ with variable recording times. Spatial and temporal frequency influences on optical memory were again evaluated as well as the damage threshold of the device.

The third and final stage in the research developed from phenomena observed in stages one and two. Here, the imaging characteristics of the conducting PRIZ were investigated and quantified over a range of spatial and temporal frequencies with a fixed energy density. Temporal frequencies were initially obtained by on/off switching of the write-beam. Object motion was then qualitatively evaluated.

IV. Experimental Procedure

This chapter describes the general experimental setup, the two types of write-beam sources used, the procedure and criteria designed to calculate maximum resolution for imaging experiments, and the procedure used to determine spatial and temporal influences on the conducting PRIZ. Results of these experiments are presented and analyzed in Chapter V.

Experimental Setup

Figure 2 displays the general experimental setup which was used throughout the research. The prefixes r, w, and v identify the read-beam path, write-beam path, and viewing components respectively. The read-beam path (r1-r6) was configured to deliver a collimated beam which was parallel to the write-beam and normally incident on the PRIZ surface. The analyzer is rotated approximately 10 degrees from the normally crossed position to account for optical activity. The mechanical shutter (r2) was typically left open during testing (continuous illumination of the read-beam on the crystal).

The electronic shutter in the write-beam path (w4) was a Uniblitz SD-10 and was capable of exposures down to one millisecond at repetition rates between DC and 40 pulses/second. Evaluation of the shutter output on a storage oscilloscope found the unit to be accurate and reproducible only down to 10 ms; thus, minimum exposures were limited to this value. The shutter provided the flexibility of evaluating temporal effects on the PRIZ merely by varying the repetition rate.

This setup differs from previous AFIT experiments on the conducting PRIZ in that a focused beam was not used to write on the crystal.

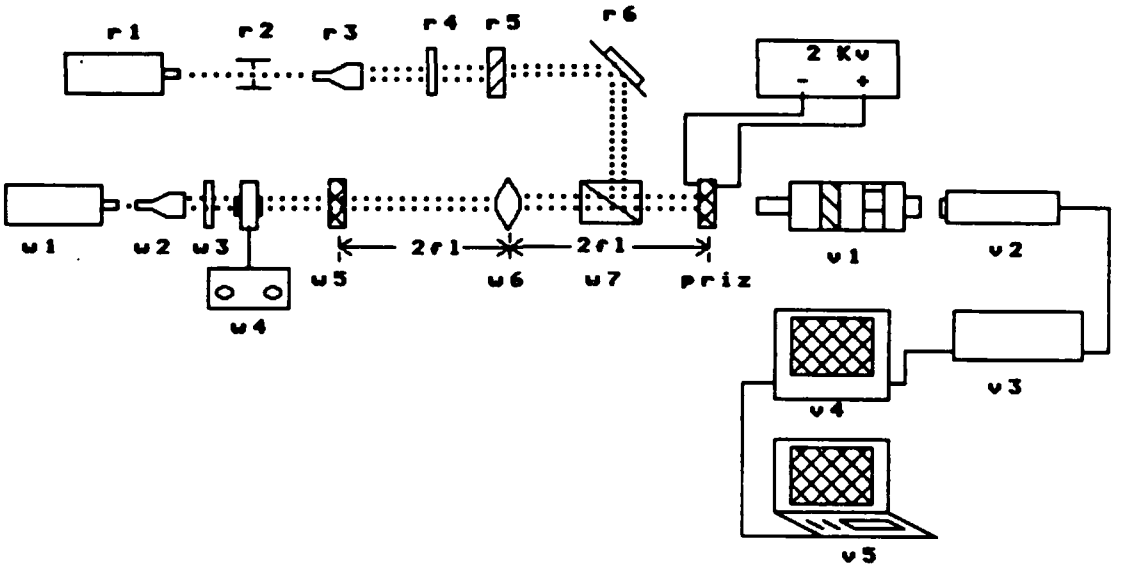

r: Read-beam path
r1: Read-beam (HeNe laser, 632.8 nm)
r2: Mechanical shutter
r3: Jodon beam expander
r4: Neutral density filter
r5: Polarizer
r6: Mirror

w: Write-beam path
w1: Write-beam source (Pressure broadened Hg source with 360-510 nm filter; or HeCd laser, 442 nm)
w2: Jodon beam expander
w3: Neutral density filter
w4: Electronic shutter
w5: Object plane
w6: Imaging lens (250 mm focal length)
w7: Polarization beam splitter

v: Viewing components
v1: Viewing optics (telescope, analyzer, 632.8 nm filter)
v2: CCD camera (Sony, Model XC-38)
v3-4: Video recorder and monitor
v5: Z-248 computer with frame grabber (Data Translation, DT2851)

Figure 2. General Experimental Setup.

Instead, an object such as the resolution test chart was imaged on the crystal with unity magnification. As in all previous experiments, the PRIZ was mounted on a Plexiglas slide with the negative electrode being the first surface to encounter the incident beams. This procedure is described in detail by Nilius (11:46-49).

The Sony CCD video camera (v2) was capable of detecting illumination as low as three lux and was convenient for evaluating low-level intensities from the PRIZ. The video monitor (v4) was connected to a Z-248 computer with a DT 2851 High Resolution Frame Grabber (v5). This package generated 480 lines at 512 pixels/line and eight bits/pixel for a single video frame. The eight bits represented one of 256 gray levels of intensity. An option existed to display an intensity profile of any line (any orientation) on the monitor. The line intensity profile was used extensively for determining maximum spatial resolution.

The nature of each experiment may have required minor variations from this general configuration. These variations included the beam expanding and collimating optics for the write-beam source, the optical density of the neutral density filters to control intensity of the write-beam and read-beam, and the additional components used to control the read-beam polarization on the crystal (for example, circular polarization required a quarter-wave plate/PRIZ/quarter-wave plate/linear polarizer arrangement).

Write-beam Sources

Incoherent imaging was achieved with an Oriel medium pressure mercury lamp. The lamp is driven by a 115 V, 2 A, 60 Hz regulated power supply. The supply output is rectified to provide 120 Hz cycling of the

lamp. The output spectrum of this source is depicted in Figure 3. Since the "useful" writing energy is contained in the 350-500 nm range, a band pass filter centered on 440nm was placed in the light path. Thus, reported energy densities for the incoherent write-beam refer to light transmitted through the band pass filter. Transmission characteristics of the filter are shown in Figure 4. It should be noted

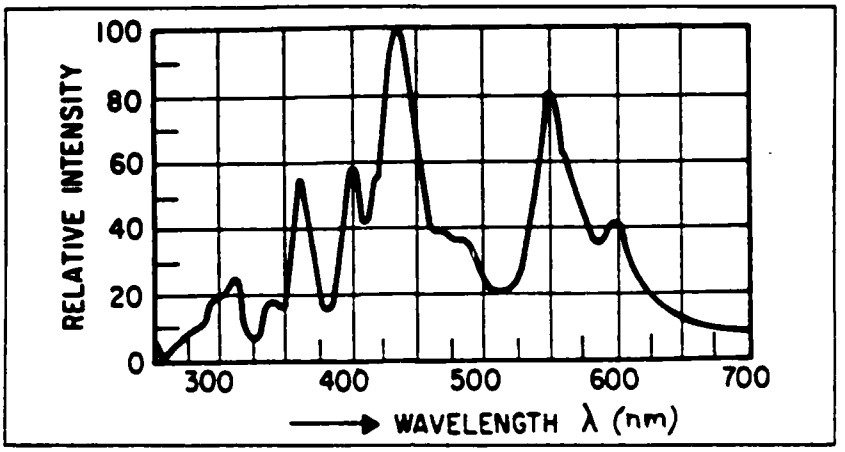

Figure 3. Spectrum of the Oriel Hg Source (18:18).

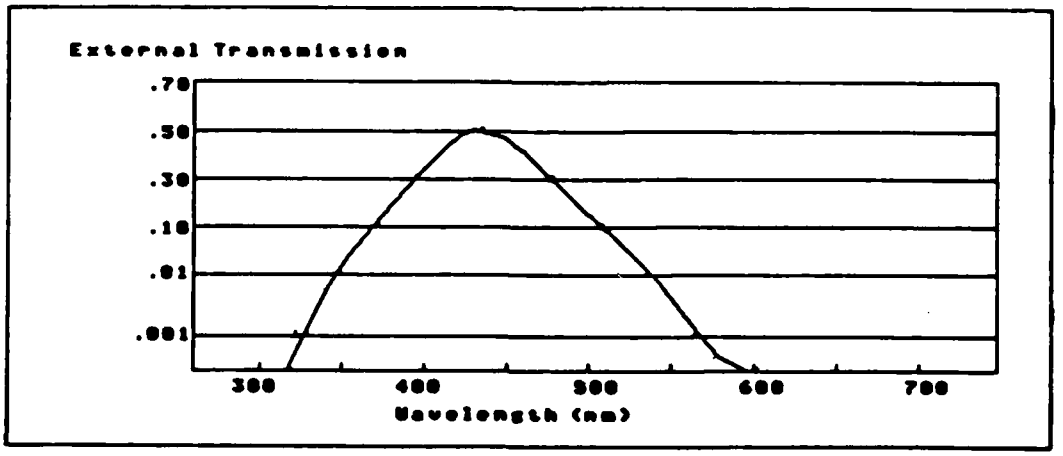

Figure 4. Transmission Curve of the 440 nm Band Pass Filter.

that the predominant lines of the mercury source in this band are at 365, 400, and 435 nm (18:18), and from Figure 4 the filter transmits approximately 10%, 40%, and 50% respectively at these wavelengths.

Coherent imaging was obtained using a HeCd laser (442 nm, 40mW). The beam was expanded and collimated to a diameter of approximately 2.5 cm. This provided more than sufficient intensity (1400 $\mu W/cm^2$) for most measurements, while providing illumination of a large region on the resolution chart using a relatively small area of the gaussian beam, so that a nearly uniform intensity distribution was measured across the imaging region.

Resolution Criteria

The resolution of an imaging system is typically described in terms of its ability to distinguish between two closely spaced point sources and is therefore related to the width of the impulse response of the system (8:507). That is, a system with a narrow impulse response has a "wide" transfer function (high cutoff frequency) which results in a high degree of resolution. The resolution of the conducting PRIZ was evaluated using a standardized USAF 1951 Resolution Test Chart placed in the object plane of the imaging lens in the write-beam path. The chart was imaged on the first surface of the crystal, and the output resolution was scored according to the smallest resolved pattern. An example of a test chart is shown in Figure 5. The resolution, R, may be computed from the equation (22:1):

$$R = 2^{k+(n-1)/6} \text{ line pairs/mm}$$

where k is a major group of charts (0,1,...,7), and n is an element

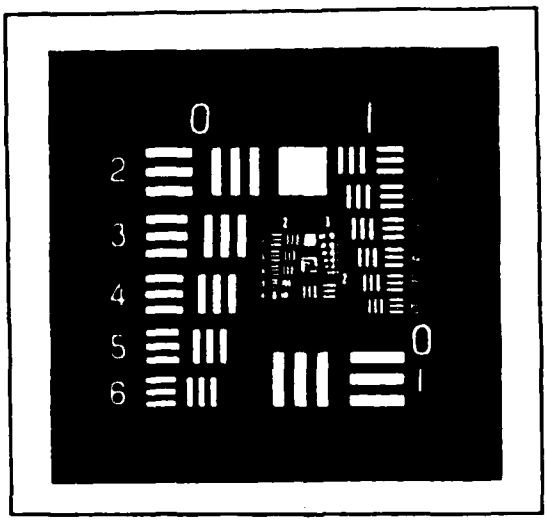

Figure 5. USAF 1951 Resolution Test Chart.

within the group (1, 2, ..., 6). For this research, groups 1-6 were used (1-114 lp/mm).

Visual determination of resolution can be very subjective, as edge contrast and general image quality become dominant factors. For this research, where coherent and incoherent imaging were to be "compared", it was essential to establish a measurable criteria which could be applied to both sources since image quality was found to be somewhat degraded in the coherent case. The criteria developed is a hybrid of video luminance ratios used in image evaluation and the Rayleigh criteria for resolution of two point sources.

Luminance ratio is merely the maximum video screen brightness divided by the minimum brightness (19:145). For this research, it refers to the ratio of an enhanced edge to its adjacent DC filtered region.

The Rayleigh criteria states that two points are just resolved when the center of the airy disk of one source falls on the first zero of the

other source (9:129). This case is shown in Figure 6. The maximum intensity is found to be 19% higher than the intensity between the two patterns. Thus, the maximum resolved pattern for this research was based on the following requirements: (1) The pattern must display three distinct nulls on a line intensity profile. This corresponds to the DC filtered regions of the three horizontal and vertical bars. On highly resolved patterns, additional nulls would exist between the edges of two adjacent bars; however, for this research it was considered sufficient if the two adjacent edges appeared as one. (2) The luminance ratio of the pattern must be greater than 1.19. Higher ratios imply better contrast. The outermost edges of a pattern typically displayed a higher intensity than inner edges. In addition, there existed an intensity

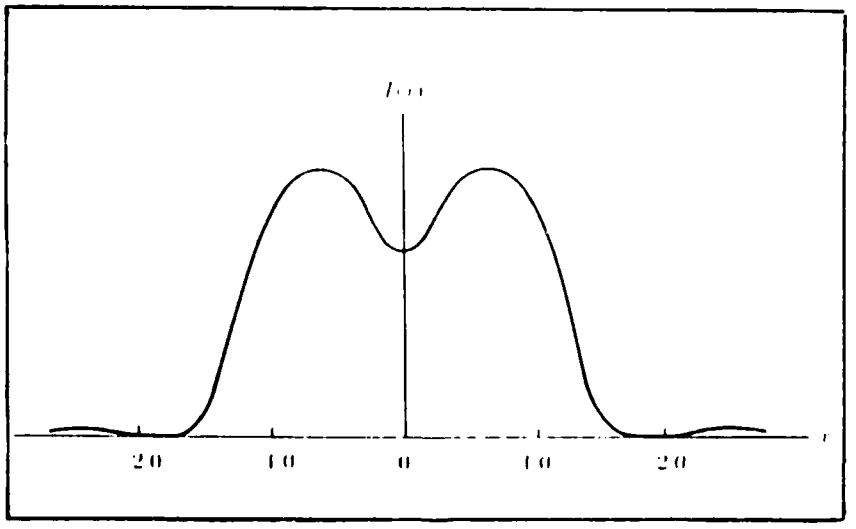

Figure 6. Image Intensity for Two Incoherent Point Sources Separated by the Rayleigh Distance (9:130).

asymmetry between the opposite edges of a bar which will be described in Chapter V. Therefore, to standardize resolution measurements, once requirement 1 was satisfied, requirement 2 was applied to the center null and its two adjacent peaks. Figure 7 illustrates two line intensity profiles from a PRIZ output. Figure 7a meets the two requirements and is considered resolved, while Figure 7b has only two nulls and thus is not resolved.

This method is unique and differs from previous resolution measurements on the PRIZ which are in terms of diffraction efficiency (15:166). It provides a means of measuring resolution in a manner which is objective, reproducible, and relatively simple.

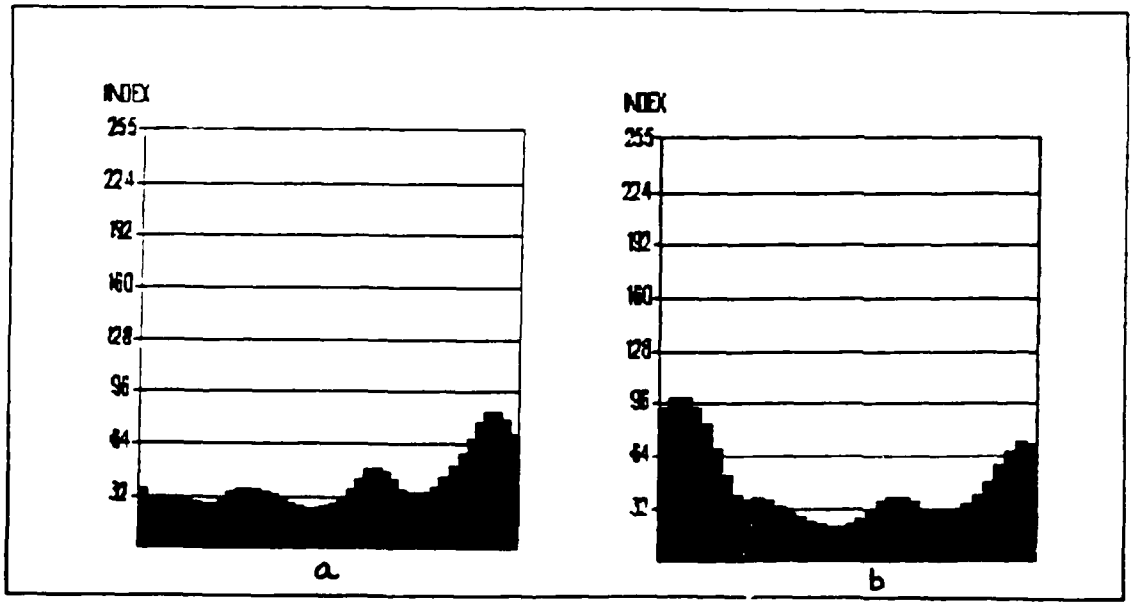

Figure 7. Line Intensity Profile of a Spatial Pattern at the PRIZ Output: a) Resolved Pattern, b) Nonresolved Pattern.

Spatial-Temporal Characteristics

Observations from the resolution experiments indicated that the temporal frequency of the input image (in this case, a single or multiple pulse) significantly influenced optical output of the PRIZ. In fact, the relatively fast output decay described in the dynamic imaging mode was found to require some nonzero temporal frequency as well as a high energy density. Therefore, a series of experiments was designed to explore the temporal influence on the conducting PRIZ.

The first experiment was intended to compare the pulsed optical output of these "carefully prepared" crystals with that reported by Nilius (11:19). Using the incoherent light source, an energy density of 5 $\mu J/cm^2$ was pulsed on the device every five seconds. Thus, the experiment was identical to Nilius' except this procedure used a low intensity write-beam from an incoherent source, and intensity was measured for various spatial frequencies.

In the next experiment, a fixed energy density from the coherent write-beam source was selected which coincided with the peak resolution data. The write-beam repetition rate was then varied on the electronic shutter over a range of 0-10 Hz while imaging the resolution test chart on the conducting PRIZ. The purpose of this testing was threefold:

1. Verify the spatial-temporal dependency of the device which controls dynamic image selection as described in the Soviet literature (15:165, 16:255, 3:692).
2. Quantify this dependency over a broad spatial frequency range (1-32 lp/mm). This data is not available in any of the literature.

3. Investigate the relationship between switching frequency and object velocity for dynamic image selection.

Additional data on write-induced damage and its associated effects on output intensity were gathered in this series. The results are reported in Chapter V.

V. Analysis of Results

Image Resolution From an Incoherent Write-beam

A graph of spatial resolution versus single-pulse write-beam energy density for the incoherent source is shown in Figure 8. This graph was generated by maintaining a fixed write-beam intensity of 4.7 $\mu W/cm^2$ and varying the open shutter time from 0.1 to 12.0 seconds. The read-beam was linearly polarized since directional filtering was not a hindrance in these measurements. Resolution was determined using the Rayleigh-type criteria described in Chapter IV.

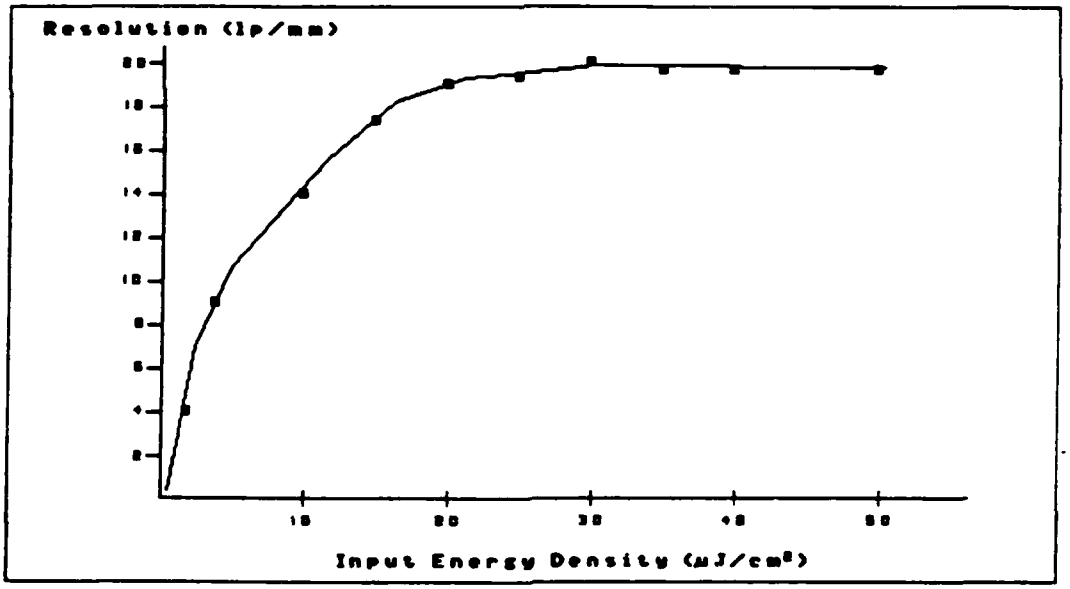

Figure 8. Spatial Resolution Versus Single-Pulse Energy Density for an Incoherent Write-beam.

From Figure 8 it can be seen that the spatial resolution of the conducting PRIZ reaches a maximum of 20 lp/mm at a total energy density of approximately 25 $\mu J/cm^2$. The resolution of the device does not improve for higher energy densities when tested at levels as high as 125 $\mu J/cm^2$. It was found that the minimum energy density required to obtain 1 lp/mm resolution was approximately 1 $\mu J/cm^2$. This is the same energy density as that specified for the sensitivity of the PRIZ in the Soviet literature (3:689), although the device type ("standard" or "conducting") and recording source type (coherent or incoherent) are not specified.

In determining spatial resolution using such a low intensity source and relatively long write times, it was not clear how the writing times affected the resolution versus energy density curve. Clarification was obtained by measuring resolution using a set of fixed intensities with variable recording times, then variable intensities with a fixed recording time. Write-beam intensities ranged from 0.31-4.7 $\mu W/cm^2$, and write times range from 0.1-99 seconds. Each test resulted in the same general curve - the resolution peaked at 20 lp/mm for an energy density of approximately 25 $\mu J/cm^2$, with a minimum resolution (1 lp/mm) observed at approximately 1 $\mu J/cm^2$. Therefore, the spatial resolution of the conducting PRIZ is apparently a function of the total write-beam energy density independent of the time required to deliver that energy for times between 0.1 and 99 seconds.

The maximum resolution of 20 lp/mm found in this study is much less than the 50 lp/mm specified in the Soviet literature (3:689). Two points are offered to clarify this apparent discrepancy. First, patterns as high as 32 lp/mm were visually resolved at the output of the

PRIZ but did not pass the specified resolution criteria. Second, it is not clear from the literature if image resolution from a low intensity, incoherent write-beam has ever been evaluated.

Additional Observations With the Incoherent Source

The resolution of the PRIZ was evaluated for the case of a circularly polarized read-beam which produces a modulated output with no directional filtering. The device peaked in the same energy density range as the linearly polarized case, but the maximum resolution was somewhat degraded (16 lp/mm). Unlike a linearly polarized beam which requires only a crossed polarizer at the PRIZ output to obtain amplitude modulation, a circularly polarized reading beam requires a quarter-wave plate / PRIZ / quarter-wave plate / analyzer configuration. Precise alignment of the fast and slow axes of the quarter-wave plates is necessary to eliminate analyzer bias, or incomplete extinction, at the output. Total extinction of the read-beam was not observed in this experiment.

The effect of polarization "quality" of the read-beam on the modulated output of the conducting PRIZ has been reported by Padden in reference 14. He shows that a nearly linear or nearly circularly polarized read-beam with some degree of ellipticity results in an asymmetry in the optical output. Padden extends earlier analyses by including the effects of natural optical activity in BSO. The visual effect of the asymmetry is an image in which one edge is brighter than the other. A purely linear or circular polarization cannot be obtained; thus, the asymmetry was observed in varying degrees throughout this research, consistent with Padden's results.

Although energy densities as high as 150 $\mu J/cm^2$ were used to record images on the conducting PRIZ, there was no indication of the relatively fast output decay which has been reported and is necessary for dynamic imaging (11:24). In fact, it was found that the optical memory of the device increased with increased energy density. For an energy density of 25 $\mu J/cm^2$, the 10% memory time, which has been defined as the length of time after writing in which the optical output of the crystal decays to a value that is 10% greater than the read-beam only output (11:21), was found to be one hour for 1 lp/mm, 51 minutes for 4 lp/mm, and 23 minutes for 16 lp/mm. The read-beam was on continuously, and though not quantified, increasing the read-beam intensity had no significant effect on optical memory. Higher energy densities resulted in equal or increased 10% memory for the higher spatial frequencies (greater than 30 minutes for 16 lp/mm at 50 $\mu J/cm^2$). This appears to contradict earlier studies in which the optical memory was shown to decrease with increased energy density (11:19), though it is re-emphasized that low intensity, incoherent write-beams were not previously tested, and spatial frequency of the input image was not considered a variable. From this data, it is apparent that the optical memory of the conducting PRIZ is a function of spatial frequency as well as energy density of an input image, and the characteristics of dynamic imaging are not observed at such low intensities for a single recording pulse.

The significance of a single-pulse write-beam requires some elaboration. An experiment was performed in which the resolution chart was recorded on the conducting PRIZ using an energy density of 5 $\mu J/cm^2$ recorded on the device every five seconds in a one second pulse width. The results are shown in Figure 9 for two spatial frequencies. For a

spatial frequency of 1 lp/mm, the output intensity peaked at 40 $\mu J/cm^2$, while the 16 lp/mm pattern peaked at 70 $\mu J/cm^2$. For all spatial frequencies, the maximum output intensity was followed by a decrease of approximately 15% to a steady output as shown for the two spatial frequencies in Figure 9. This is similar to the results reported by Nilius where a spatial frequency of approximately 1 lp/mm must be assumed. The output characteristics for a multiple-pulsed write-beam, when compared with the single pulse data, verify the existence of an additional variable in dynamic image selection - the temporal frequency of the input image. In this case, temporal frequency refers to the switching rate of the electronic shutter (0.2 Hz). The combined influence of energy density, spatial frequency, and temporal frequency on dynamic image selection is dedicated to a later section in this chapter.

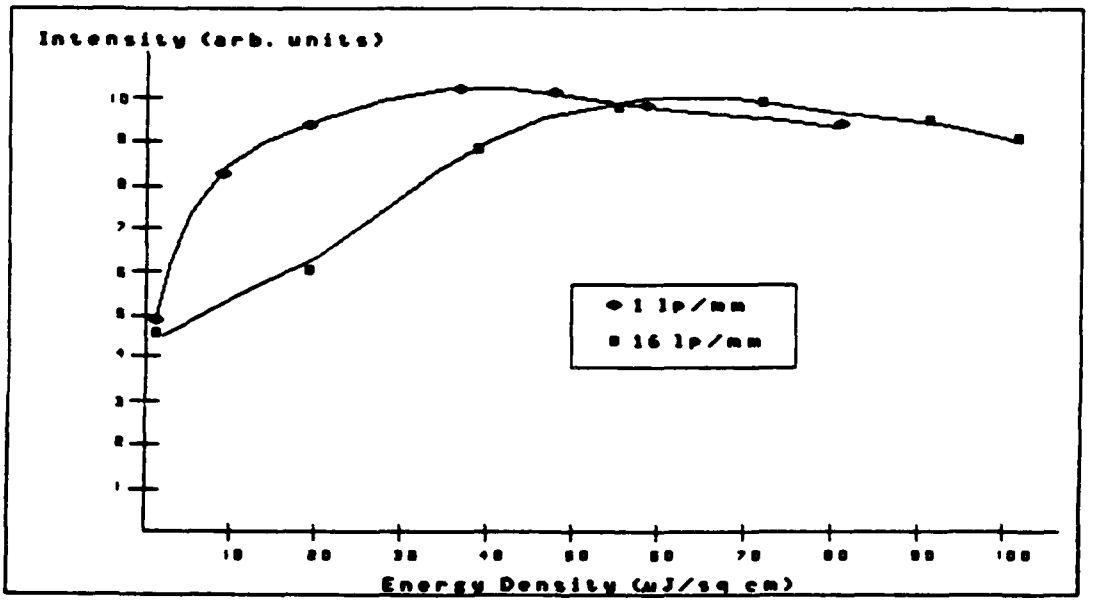

Figure 9. Pulsed Optical Output (5 $\mu J/cm^2$, 0.2 Hz).

Image Resolution From a Coherent Write-Beam

The spatial resolution of the conducting PRIZ using the HeCd laser as a write-beam source was measured using the same procedure as that which generated the data on the incoherent source appearing in Figure 8. That is, the energy density was varied by using a fixed intensity with variable recording times. It was noted that the visual quality of the image was poorer for coherent imaging. This is attributed to the effects of diffraction patterns and reflections which were superimposed on the image and degraded the modulated output of the crystal.

Spatial resolution as a function of single-pulse energy density is shown for the coherent source in Figure 10. The maximum resolution of the conducting PRIZ for this type of recording source is 40 lp/mm at a minimum energy density of approximately 90 $\mu J/cm^2$. The resolution does not improve for higher energy densities when tested at levels as high as 1150 $\mu J/cm^2$ which is shown in a later section to be the damage threshold range of the device. As in the case of incoherent imaging, higher spatial frequencies were visually resolved but did not meet the resolution criteria. For this experiment, patterns as high as 50 lp/mm were visible, which is precisely the spatial resolution specified in the Soviet literature for the "general" PRIZ spatial light modulator (3:689). In addition, the minimum energy density required for 1 lp/mm resolution was determined to be 2 $\mu J/cm^2$.

A significantly higher intensity was available for coherent imaging (135 $\mu W/cm^2$); thus, to re-evaluate the influence of writing times on output resolution, the coherent write-beam was filtered down to an intensity of approximately 5 $\mu W/cm^2$, and spatial resolution was evaluated over an energy density range of 5-32 $\mu J/cm^2$. Again, it was

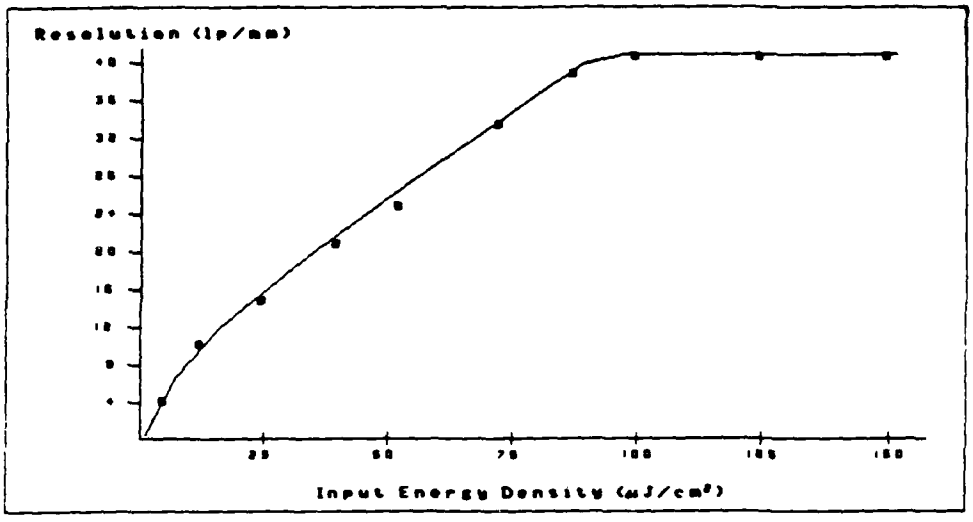

Figure 10. Spatial Resolution Versus Single-pulse Energy Density for a Coherent Write-beam.

determined that the spatial resolution of the conducting PRIZ is a function of the total (integrated) energy density and not the intensity of the write-beam.

A comparison of the spatial resolution of the conducting PRIZ for the two types of recording sources (Figures 8 and 10) reveals some interesting results. First, the maximum resolution from the coherent write-beam is twice that of the incoherent source (40 lp/mm and 20 lp/mm respectively), although the necessary energy density to obtain this resolution is also substantially higher (90 $\mu J/cm^2$ and 25 $\mu J/cm^2$ respectively). Second, for energy densities less than 30 $\mu J/cm^2$, the spatial resolution for a given energy density is higher for the incoherent source. For example, at an energy density of 10 $\mu J/cm^2$, the resolution from the incoherent source is 14 lp/mm while that from the coherent source is 9 lp/mm. Finally, for both sources, a maximum resolution is obtained at a certain energy density, then does not

improve or degrade with additional energy deposited. This result signifies an apparent saturation of the transverse fields within the crystal. At this point, there is no obvious explanation for the difference in resolution from the two write-beam sources.

Additional Observations With the Coherent Source

As with the incoherent source, fast output decays, typical of that predicted for high energy density write-beams, were not observed for single-pulse exposures below the damage level of the crystal. Energy densities as high as 250 $\mu J/cm^2$ were written on the device, and the optical output, though not quantified, remained for long times (order of many minutes) as with previous measurements. However, multiple pulses of the recording image produced decaying images similar to that observed with the incoherent source, and these effects are addressed in the last section of this chapter.

Crystal damage was observed during coherent imaging at high energy densities and is described in the next section.

Write-Beam-Induced Damage

Crystal damage is reported prior to an analysis of spatial-temporal influences on the dynamic imaging mode since, as will be discussed, the output characteristics of the conducting PRIZ in localized regions of surface layer damage are similar to that observed in dynamic imaging.

Catastrophic damage similar to that described by Anderson (1:4.8) was first observed during high energy density recording when the electronic shutter was inadvertently left open longer than desired. The damage was in the form of symmetric, three-bladed propeller patterns which were dispersed over most of the negative surface of the crystal.

On the video monitor, these patterns appeared as lines in the crystal with very bright edges and dark troughs. At the time, the total energy density of the input image was known only to be in excess of 1000 $\mu J/cm^2$, but several interesting phenomena were observed when the video tape was replayed using a single frame advance. Since the frame rate of the video recorder is 30 sec^{-1}, this option allows viewing of 33.3 msec windows. Unfortunately, the 632.8 nm filter was inserted so that the write-beam image could not be observed along with the modulated output or energy density could have been computed.

First, at the same time that a crack was initially observed at the output of the crystal, the output image faded to a level just above the read-beam background intensity. The image did not return in subsequent frames. The image transformation can be described as follows: Several frames prior to the visible damage, the DC spatially filtered region where the crack will appear shows random areas of increased intensity. At the onset of a visible crack, the enhanced edges decay "instantaneously" (in the same video frame). These effects are observed only in the immediate region of the damage. Second, the initial damage originated in a square on the bar chart which had a width of 0.5 mm, equivalent to the width of a bar in a 1 lp/mm spatial frequency. The lowest spatial frequency being observed at the time was 4 lp/mm. Resolution at the higher spatial frequencies was unaffected by the initial damage which steadily propagated through the lower spatial frequencies.

Following this experiment, intentional damage on the crystal was induced in order to quantify the damage characteristics. In one exposure, catastrophic damage was observed at an energy density of 1150

$\mu J/cm^2$ and originated on the 1 lp/mm pattern. A second exposure in the same region of the crystal resulted in damage at 1430 $\mu J/cm^2$ on a 2 lp/mm pattern. In both cases, the output intensity of the bars in the local region of the damage was reduced to a level just above the read-only level in the same frame that initial cracks were observed. After a total energy density of 2015 $\mu J/cm^2$ had been deposited, the spatial patterns between 23 lp/mm and 40 lp/mm were still visually resolvable, while the lower spatial frequency patterns had decayed to various intensity levels. The high frequency patterns were still visible 12 minutes after writing until gross damage propagated into that region.

These preliminary results indicate that the damage threshold of the conducting PRIZ is a function of both the write-beam energy density and spatial frequency of the input image, and the general range of damage occurs between 1150 and 1430 $\mu J/cm^2$ for low spatial frequencies, while the device appears to tolerate greater than 2000 $\mu J/cm^2$ for spatial frequencies above 23 lp/mm.

How do damage levels on the "carefully prepared" crystals compare with damage reported on previous AFIT crystals? Since spatial frequency was not considered a variable in previous research, it is difficult to compare unless low spatial frequencies are assumed (recall that previous researchers used focused write-beams which had gaussian profiles). Anderson reports damage similar to that observed in this research to occur after a three second exposure with a write-beam intensity of 293 $\mu W/cm^2$ (1:4.5). In Shield's demonstration of dynamic imaging, a "CORNELL" image was reported to disappear after two seconds of writing at approximately 500 $\mu W/cm^2$ (20:45). This test was later shown to cause catastrophic damage to the crystal. Thus, although precise energy

densities cannot be computed as the beams were nonuniform, damage may be estimated to have occurred in the range of 1000 $\mu J/cm^2$. Therefore, the specially prepared crystals used in this research appear to be slightly improved over previous AFIT crystals in terms of damage threshold. Finally, Anderson reports extensive damage on the crystals used by Nilius in the form of electrode damage, crack damage, striations, and pit damage (1:4.22), but specific energy levels are not available.

Can surface layer damage like that reported in this research go unnoticed? When regions of sparse damage were illuminated with a read-beam of relatively high intensity (0.3 mW/cm^2) with the external voltage applied, the cracks were very bright and continued to propagate across the crystal even though no write-beam was being applied. This observation may explain Casasent's statement that the lifetime of the PRIZ is a concern when operated at "high read-beam irradiances" (6:3848). The read-beam does not appear to initiate damage; however, it does propagate existing damage in the crystal. When the read-beam is sufficiently reduced, the existing damage does not appear to propagate, and if relatively sparse, can even go unnoticed unless a highly light sensitive camera is used. This was qualitatively verified by reducing the read-beam intensity to 25 $\mu W/cm^2$, placing a neutral density filter in front of the Sony CCD video camera, and viewing damaged regions on the crystal.

Therefore, some of the previous demonstrations of dynamic image selection in the conducting PRIZ may have actually been a result of write-beam-induced damage. Data presented in the next section suggest that this must indeed be the case when a single-pulse write-beam is used on a stationary image.

Spatial-Temporal Characteristics

Soviet literature has alluded to the controlling variables in the dynamic image selection (DIS) mode of the PRIZ spatial light modulator, but the information is typically incomplete or ambiguous. For example, Petrov reports that the effect of DIS manifests itself only at fairly high energies of recording light (17:169). Nilius expanded on the energy dependence by quantifying the optical memory of the device as a function of write-beam energy density; however, this thesis shows that Nilius' numbers are applicable only to multiple-pulse write-beams and vary with the spatial frequency of the input image. As a second example, Petrov reports a spatial-temporal frequency influence on the modulated output of the PRIZ and states that a decrease in spatial frequency of an image is accompanied by a shift of the maximum diffraction efficiency of the modulator toward a higher temporal frequency (15:165). This spatial-temporal dependency is reproduced in Figure 11. No specific numbers are reported with regard to energy density or spatial frequency, but Figure 11 implies that the diffraction efficiency for all spatial frequencies is zero when the temporal frequency is zero. This suggests, and is affirmed by Petrov, that the output of a stationary image is suppressed even when no temporal variation is present in the recording light (on/off switching or sinusoidal variation). As previously mentioned, that output phenomenon was only observed in this thesis when the energy density for a given spatial frequency was at the damage threshold of the device. Therefore, the objective of the final section of this thesis is to identify and quantify the variables which control DIS in the conducting PRIZ based on observations in this research.

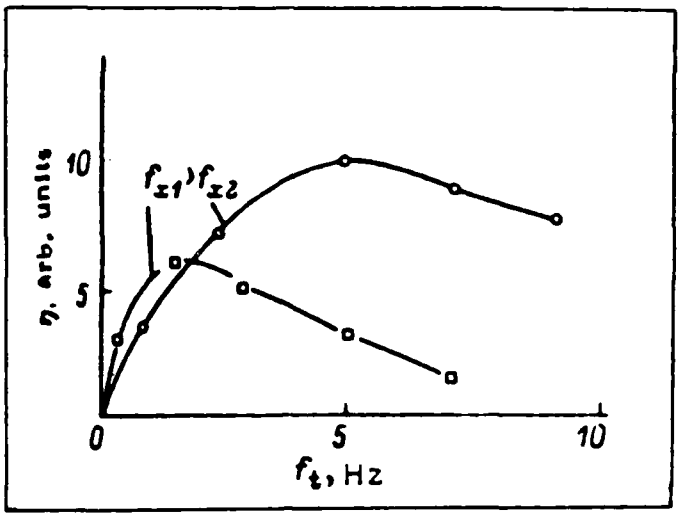

Figure 11. Dependence of Diffraction Efficiency as a Function of Temporal Frequency (15:165).

As was shown earlier, the optical memory of the device was relatively long when single-pulse write-beams were used at energy densities up to the damage threshold of the crystal. However, multiple pulses were shown to cause an output decay, characteristic of that described in dynamic imaging. The first task in this series of experiments was to quantify the spatial-temporal dependence shown in Figure 11 for a specific energy density following the procedure described in chapter four. The results of this experiment are presented in Figure 12 and were obtained with an energy density of 10 $\mu J/cm^2$ per pulse at a pulse width of 40 msec. Total pulses were limited to 12 (for a total energy density of 120 $\mu J/cm^2$) to avoid damage levels, yet provide sufficient total energy density to record all spatial patterns. It can be seen that this energy density was inadequate to achieve a

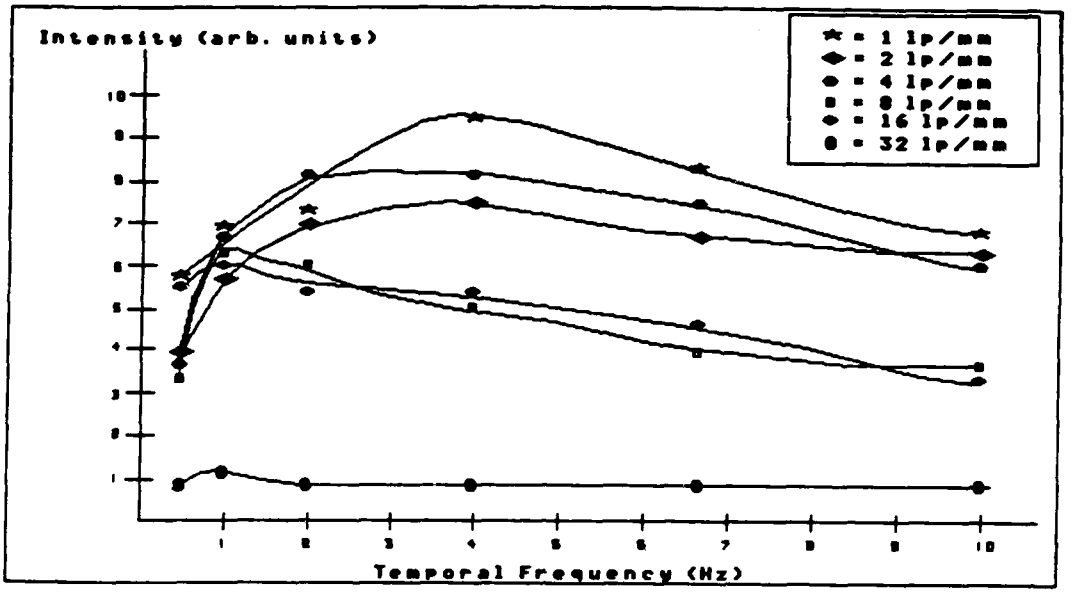

Figure 12. Relative Output Intensity Versus Temporal Frequency for Various Spatial Frequencies.

relatively high output intensity at 32 lp/mm, although a peak intensity was still identified.

Figure 12 verifies the inverse relationship between spatial and temporal frequencies with respect to peak output intensity. That is, a decrease in spatial frequency is accompanied by a shift of the peak output intensity toward a higher temporal frequency. This relationship may be summarized in a plot of the maximum output intensity for a given spatial and temporal frequency as shown in Figure 13. Here it is seen that the temporal frequency ranges from 1-4 Hz for spatial frequencies between 32 and 1 lp/mm.

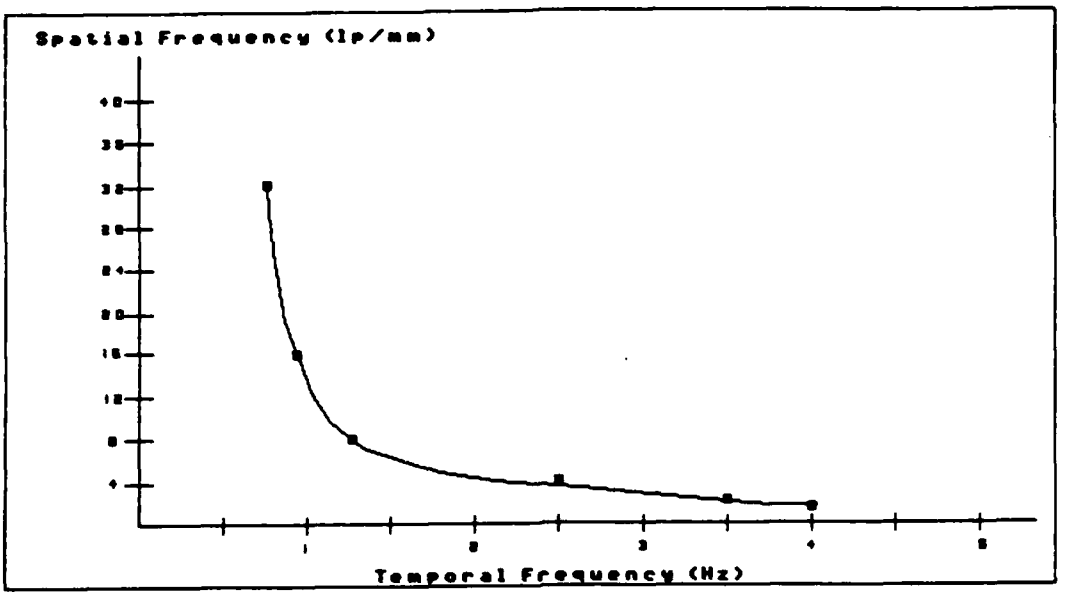

Figure 13. Maximum Output Intensity for Spatial Frequency Versus Temporal Frequency.

Figures 12 and 13 suggest that the output intensities for all spatial frequencies are nonzero for a DC temporal frequency (single-pulse write-beam or stationary object) if the energy density is sufficient to record the spatial pattern. This, in fact, was demonstrated during the coherent resolution measurements when single-pulse write-beams were used with energy densities ranging from 1 $\mu J/cm^2$ to the damage threshold of the crystal, and relatively long optical memory was observed. In addition, Figure 13 shows that a maximum output intensity may be obtained for very low temporal frequencies at very high spatial frequencies, although it was shown that the spatial resolution of the conducting PRIZ saturates at 40 lp/mm when using the HeCd laser for a write-beam.

It must be re-emphasized that the numbers in Figures 12 and 13 are for a specific energy density (per pulse and total). Results from Nilius' research indicate that the numbers will change as energy density changes. The next experiment in this series demonstrates that assertion for a specific spatial frequency of 4 lp/mm and temporal frequency of 1.25 Hz. First, a write-beam energy density of 25 $\mu J/cm^2$/pulse was used. After the first pulse, a bright edge-enhanced output was observed as was anticipated based on the energy density required to resolve 4 lp/mm (Figure 10). The average output intensity increased with the first five pulses (125 $\mu J/cm^2$ total energy density) except a temporary suppression of the output by about 5% was observed in the same video frame that the second through fifth pulses were delivered. Following the fifth pulse, and consistent with the pulsed data presented in Figure 9, the output decreased to a steady value which was approximately 10% below the maximum intensity, with no additional suppression observed. Next, the write-beam was increased to 90 $\mu J/cm^2$/pulse. The same effect was observed as with the lower energy density except the output intensity was decreased by approximately 75% following the second pulse. The third pulse on the device had no apparent effect; that is, it caused no additional suppression or intensification, similar to the previous case for pulses beyond the fifth pulse. This data implies that a higher energy density will generally result in an increased suppression of stationary images, which is precisely what Nilius concluded; however, Nilius implies that a single pulse is adequate, while this report establishes the requirement of a multiple-pulse write-beam.

The correlation between a pulsed write-beam on a stationary image and a continuous write-beam on a moving image is not obvious. Petrov

reported that the response of the modulator to a 0.5 mm input line was measured for velocities of 1-40 mm/sec across the input plane and found that the intensity peaked at a velocity of 7 mm/sec (15:166). Since this peak velocity is dependent on energy density, and no value for energy density is reported, a direct comparison cannot be made with Figure 12. However, for a given energy density and spatial frequency, the trend reported by Petrov is identical to that shown in Figure 12; that is, a peak output intensity occurs at a specific temporal frequency with some level of intensity suppression for other temporal frequencies. Again, Petrov reports a significantly reduced output intensity when the velocity, or temporal frequency, is zero, and that effect was not observed in this research when the energy density was sufficient to record the spatial pattern yet below the damage threshold of the crystal.

As a final demonstration of the dynamic imaging mode, a silhouette of a tank was placed in the object plane of the write-beam path and imaged on the surface of the conducting PRIZ. The purpose of this experiment was to demonstrate DIS of an object consisting of various spatial extents and dimensions. A video frame of the tank image as it appeared on the crystal surface is shown in Figure 14. The maximum height of the tank is 1 mm, the length is 2.5 mm, and the width of the gun barrel is approximately 0.15 mm. First, a stationary tank image was recorded on the PRIZ using a single-pulse write-beam with an energy density of 140 $\mu J/cm^2$. This value was selected since it is 1.5 times greater than the saturation energy for coherent resolution, and is well into the range reported to produce high output decay rates (11:24). The image was rotated to minimize the directional suppression which is

in the horizontal direction. The modulated output was a bright, edge-enhanced image with suppression confined only to the regions of directional filtering and appears in Figure 15.

Next, a moving tank image was recorded on the device using the same energy density. The image was manually translated across the plane so that the velocity was neither constant or calibrated; however, velocities could be approximated in segments of the recording using the frame advance of the video recorder (30 frames/sec) and the DT 2851 Frame Grabber. Over 4 mm of total travel, the velocity was estimated to vary from 0-3 mm/sec. As the image moved across the PRIZ, the modulated output of the leading edge was constantly visible, with the barrel (highest spatial frequencies) being the first structure to be degraded as the velocity was increased. In addition, the top and bottom edges of the image were visible across the video screen giving the appearance of a trail. However, all regions behind the path of the leading edge were completely suppressed (to the read-beam only level). A sequence of video frames of the modulated output is shown in Figure 16.

Temporal frequency data presented in this thesis would suggest that the areas of output suppression were due to a re-writing over the initial input image. This may be visualized as a sequence of recordings across the image plane of the PRIZ. All regions of the crystal which were imaged on in the "previous recording" will be suppressed in "subsequent recordings". This is equivalent to writing with a multiple pulse. The trail is due to the fact that the top and bottom edges are imaged at a different location with "each recording," and there is no re-writing which implies a single-pulse write-beam at each point

Figure 14. Original Input Image of Tank.

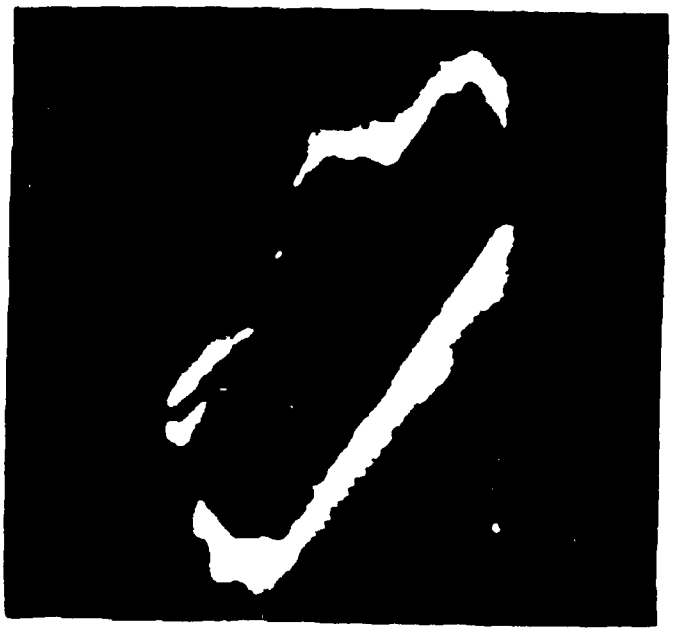

Figure 15. Edge-Enhanced Image of Tank at Output of PRIZ.

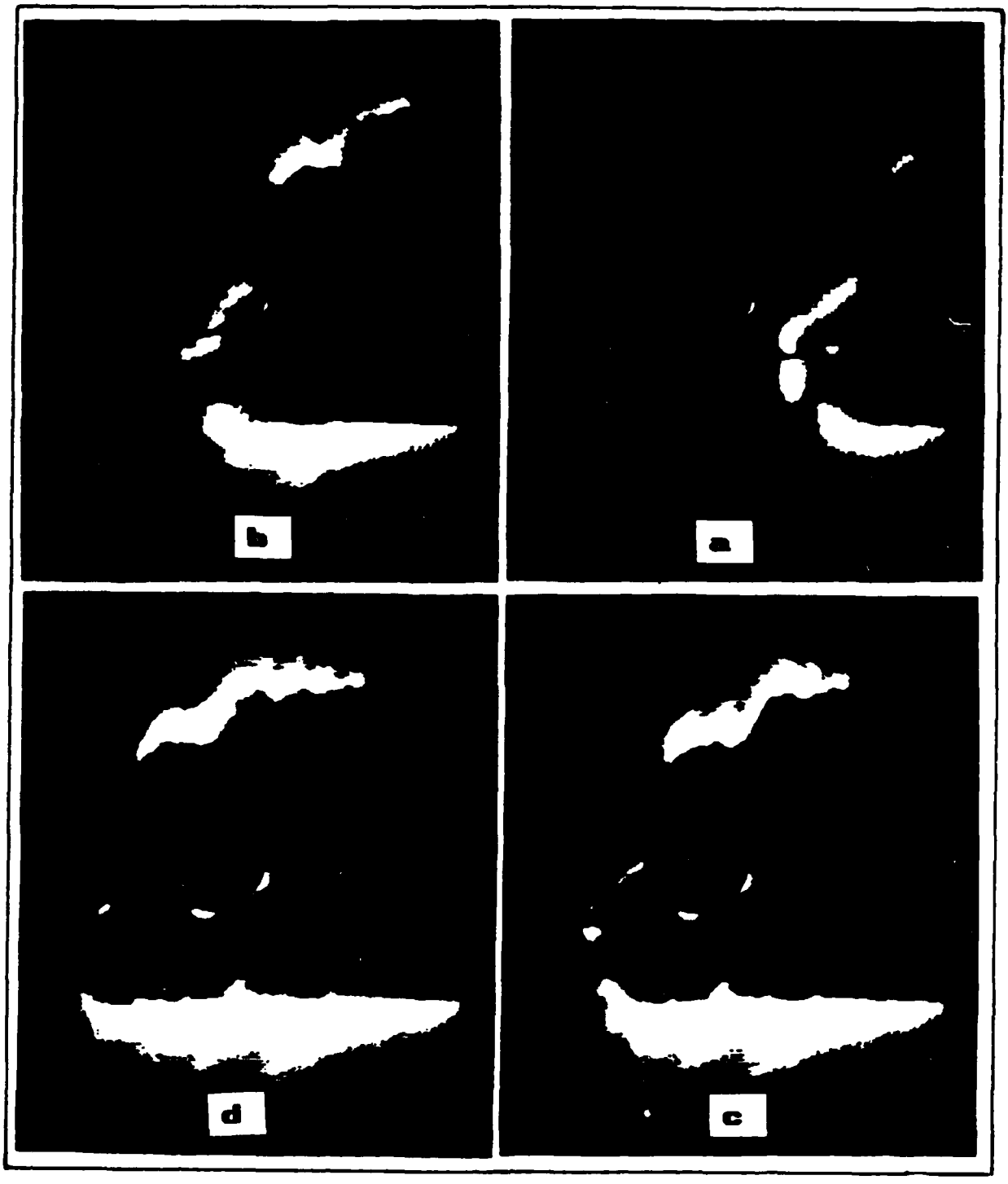

Figure 16. Sequential Video Frames of Moving Tank at Output of Conducting PRIZ.

accompanied by a relatively long memory.

Casasent et al quantified the amount of background suppression obtained as the intensity of a moving spot was varied. The results are reproduced in Table 2, where the ratio

$$R = \frac{\text{intensity of moving spot}}{\text{average intensity of fixed background}}$$

was measured at the input and output of the system (6:3854).

Table 2. Quantitative Dynamic Image Selection Data on the (Soviet) Priz (6:3854)

R_{in}	1	2.5	10	25
R_{out}	5	50	48	49

Consistent with other observations in this thesis on the DIS mode of the conducting PRIZ, the results in Table 2 must be for a specific spatial frequency, temporal frequency (velocity), and energy density of the input image. Therefore, the maximum r_{out} of 50 which is reported in Tables 1 and 2 is for one set of values consisting of a 40 μm spot being scanned at 2.8 mm/sec (6:3853).

For the imaging experiment on the moving tank, a fixed background was not used; thus, a direct comparison cannot be made with the degree of background suppression reported by Casasent. However, a new ratio, R', is provided where

$$R' = \frac{\text{intensity of output leading edge}}{\text{intensity of output trailing edge}}$$

The intensity of the leading edge at a specific point and time is dependent on the velocity of the image (corresponding to the temporal frequency of the write-beam) and the local spatial characteristics. The intensity of the trailing edge is at a maximum value in the static mode and is then suppressed to some value when motion is initiated. A sample of some R' ratios from the moving tank experiment is presented in Table 3 for four different velocities. For the case of zero velocity (static image), the difference between leading and trailing edge intensities reflects asymmetry in the output image. Note that the trailing edge is suppressed to a nearly constant intensity level, found to be at or slightly below the read-only level, for all nonzero velocities. For a relatively low spatial frequency (tank body) and a low (nonzero) velocity, high ratios are obtained. The low velocity implies a high energy density write-beam on the leading edge and suppression of the trailing edge, consistent with the spatial-temporal data. The gun barrel corresponds to a higher spatial frequency than the tank body; thus, although the level of trailing edge suppression is equivalent, a

Table 3. R' Data on Moving Tank Experiment

Velocity (mm/sec)	0	0.5	1.5	2.5
R' (body)	170/148	90/4	107/5	34/5
R' (gun)	128/70	16/5	6/5	6/6

higher energy density write-beam or lower velocity is required to obtain R' levels on the gun barrel equivalent to that observed on the tank body. For example, at 2.5 mm/sec, the leading edge intensity of the tank body is reported as 34 units, while an equivalent leading edge intensity on the gun barrel occurs at a velocity between 0.5 and 1.5 mm/sec. This is again consistent with the spatial-temporal data presented in this thesis.

VI. Summary

The imaging characteristics of the conducting PRIZ were evaluated on a set of "carefully prepared" BSO crystals. Spatial resolution of the device was quantified as a function of energy density for both incoherent and coherent write-beam sources. The damage threshold of the "carefully prepared" crystals was then identified in terms of write-beam energy density and compared to damage levels reported on previous AFIT devices. Finally, the influence of temporal frequency of an input image on the PRIZ output was reported for various spatial frequencies at a fixed energy density. The effect of energy density on the PRIZ optical memory was previously quantified by Nilius (spatial and temporal frequencies neglected), while the Soviet literature has reported, though not quantified, the relationship between spatial and temporal frequencies on the PRIZ output (energy density neglected). This thesis has presented a more complete description of the optical memory features, specifically in the dynamic imaging mode by quantifying the spatial-temporal frequency influence as well as the effect of write-beam energy density on the output of the conducting PRIZ.

Conclusions

Using the model described in chapter four, the maximum spatial resolution of the conducting PRIZ was found to be 20 lp/mm for an incoherent write-beam source consisting of a pressure broadened mercury lamp with a 360-510 nm band pass filter, while the resolution was determined to be 40 lp/mm for a coherent source consisting of a HeCd laser at 442 nm. The minimum energy density required for maximum

resolution was 25 $\mu J/cm^2$ and 90 $\mu J/cm^2$ for the incoherent and coherent sources respectively. The incoherent source provided higher spatial resolution than the coherent source when operated at energy densities less than 30 $\mu J/cm^2$.

For image processing applications which require relatively long optical memory such as an image correlator, either type of write-beam source is suitable when operated in a single-pulse mode. In both cases, the minimum energy density required to obtain maximum resolution is at least an order of magnitude below the damage threshold of the device.

The controlling variables in dynamic image selection (DIS) were shown to be the spatial and temporal frequency of the input image as well as the write-beam energy density. For a specific image such as the tank described in chapter five, the spatial frequency may be considered as a "constant". Then an energy density may be selected to obtain a desired level of background suppression at a given input velocity. The pulsed optical output in Figure 9 showed that the degree of output suppression may be controlled by the level of write-beam energy density for a specific spatial frequency. Thus, if some form of thresholding is incorporated into a moving target indicator so that less background suppression can be tolerated, lower energy densities are possible which may help preclude reaching damage levels in the crystal.

The results of this thesis indicate that some non-zero temporal frequency in the input image must be present in order to observe DIS. A stationary image will not be suppressed if the write-beam is not varied in time. Furthermore, when a portion of the image is moving, only the background in the path of the moving object will be suppressed (regions

of multiple-pulse recording). Therefore, the net effect is one of target enhancement rather than background suppression when the only temporal variation in the write-beam path is due to movement. The DIS mode as described in the Soviet literature is best observed when the write-beam is continuously pulsed at some selected frequency. In this mode, the stationary portions of the entire image will be suppressed to some level, while the moving portion will be continuously visible. Of course, both the background suppression and intensity of the moving image will ultimately depend on the write-beam energy density.

Although the damage threshold of the conducting PRIZ places limitations on its use, especially in the DIS mode, these limitations may be overcome. If the write-beam is continuously pulsed, uniform illumination at the write-beam wavelength (an erase signal) may be periodically introduced before the energy density on the crystal accumulates to damage levels. On the first pulse following an erase signal, the entire image will be visible, but the stationary portions will then be suppressed on the next and subsequent pulses.

Recommendations

The most promising feature of the conducting PRIZ is its capability to discriminate between stationary and moving images in an input scene. Following the results of this thesis, the next logical step would be to design a "realistic" moving target indicator. Considerations in such a design would include write-beam energy density and repetition rate (multiple-pulse mode), erase cycles to prevent energy accumulation to damage levels, read-beam intensity and polarization, and the spatial and temporal characteristics of "anticipated" moving targets. Ideally, the

system would be designed to operate at television frame rates. In this manner, object motion could be monitored by tracking changes in pixel intensity with each successive frame.

The requirement for a non-zero temporal frequency of an input image in order to observe DIS was developed in this thesis. However, the mechanism involved which causes an image to be visible in a first pulse and suppressed in subsequent pulses is not understood. An analysis of the dynamics which cause this output phenomenon is recommended. In addition, the degree of output suppression as a function of write-beam pulse width (for a specific energy density) and delay time between pulses was considered but not completed in this research due to time limitations. This would be an interesting area to investigate.

Bibliography

1. Anderson, Danny L. Analysis of Write-Beam-Induced Damage on the Conducting PRIZ. MS Thesis GEP-86D-1. School of Engineering, Air Force Institute of Technology (AU), Wright-Patterson AFB OH, (December 1986).

2. Anderson, Danny L. and Theodore E. Luke. "Write-Beam-Induced Crystal Damage in the Conducting PRIZ," Optics Communication, 63 (2): 78-80 (July 1987).

3. Berezhnoi, A. A. and Yu. V. Popov. "Spatial-Temporal Electrooptic Light Modulators for Optical Information Processing Systems," The Optical Society of America: 684-694 (1985).

4. Casasent, D. et al. "Soviet PRIZ Spatial Light Modulator," Applied Optics, 20 (18): 3090-3092 (September 1981).

5. Casasent, D. et al. "Test and Evaluation of the Soviet PROM and PRIZ Spatial Light Modulators," Applied Optics, 20 (24): 4215-4220 (December 1981).

6. Casasent, D. et al. "Applications of the PRIZ Light Modulator," Applied Optics,21 (21): 3846-3854 (November 1982).

7. Fisher, Robert A. Optical Phase Conjugation. New York: Academic Press, 1983.

8. Gaskill, Jack D. Linear Systems, Fourier Transforms, and Optics. New York: John Wiley & Sons, 1978.

9. Goodman, Joseph W. Introduction to Fourier Optics. San Francisco: McGraw-Hill Book Company, 1968.

10. Gunter, P. "Holography, Coherent Light Amplification, and Optical Phase Conjugation with Photorefractive Materials," Physics Reports, 93 (4): 199-299 (1982).

11. Nilius, Mark E. Measurement and Analysis of the Memory Capabilities of the Conducting PRIZ. MS Thesis GEO-85D-3. School of Engineering, Air Force Institute of Technology (AU), Wright-Patterson AFB OH, (December 1985).

12. Nilius, Mark E. and Theodore E. Luke. "Memory and Dynamic Imaging in a Conducting PRIZ," Optics Communications, 57 (6): 385-386 (April 1986).

13. Owechko, Y. and A.R. Tanguay, Jr. "Theoretical Resolution Limits on Electrooptic Spatial Light Modulators. II. Effects of Crystallographic Orientation," Journal of the Optical Society of America, 1: 644-652 (June 1984).

14. Padden, Richard J. Optical Activity and its Influence on Photorefractive Material. MS Thesis GEO-88D-4. School of Engineering, Air Force Institute of Technology (AU), Wright-Patterson AFB OH (December 1988).

15. Petrov, M. P. et al. "Transients in a Space-Time Light Modulator," Soviet Technical Physics Letters,1 (4): 165-166 (April 1980).

16. Petrov, M. P. and A. V. Khomenko. "Space-Time Modulator Characteristics of Optical Transducers," Optics Communications,37 (4): 253-255 (May 1981).

17. Petrov, M. P. "Electrooptic Photosensitive Media for Image Recording and Processing," Current Trends in Optics: 161-172 (1981).

18. Pressley, Robert J. Handbook of Lasers. Cleveland: The Chemical Rubber Co., 1971.

19. Ravich, Leonard E. "Evaluation of Electronic Images," Laser Focus/Electro-optics: 145-155 (June 1988).

20. Shields, Duncan M. Construction and Analysis of a PRIZ Spatial Light Modulator Exhibiting Dynamic Image Selection. MS Thesis GEO-84D-4. School of Engineering, Air Force Institute of Technology (AU), Wright-Patterson AFB OH, (December 1984).

21. Shields, Duncan M. and Theodore E. Luke. "Operation of a Conducting PRIZ," Optics Communication,55 (6): 391-392 (October 1985).

22. USAF 1951 Resolution Chart Data, Nomenclature and Specifications. (Original Design for USAF Under Contract No. 680-66-SA-10). Buckbee-Mears Company, St. Paul, Minn., undated.

Vita

Captain Patrick Gardner [redacted] He enlisted in the Air Force in 1974 and served four years as a medical laboratory technologist. He worked a total of seven years as a medical technologist in both military and civilian hospitals before pursuing a career in electrical engineering. He received an Associate of Arts degree in Pre-Engineering from Hillsborough Community College, Florida in 1981 and a Bachelor of Science degree in Electrical Engineering from the University of Florida in 1984. During his senior year at Florida, he re-entered the Air Force through the College Senior Engineering Program. He attended Officer Training School in San Antonio, Texas and received his commission in November 1984. He then served as a Flight Control Engineer in the Aeronautical Systems Division at Wright-Patterson AFB, Ohio until reporting to the School of Engineering at the Air Force Institute of Technology as a Master of Science degree candidate in Electrical Engineering. [redacted]

UNCLASSIFIED

SECURITY CLASSIFICATION OF THIS PAGE

REPORT DOCUMENTATION PAGE

Form Approved
OMB No. 0704-0188

1a. REPORT SECURITY CLASSIFICATION UNCLASSIFIED	1b. RESTRICTIVE MARKINGS
a. SECURITY CLASSIFICATION AUTHORITY	3. DISTRIBUTION / AVAILABILITY OF REPORT Approved for public release; distribution unlimited.
2b. DECLASSIFICATION / DOWNGRADING SCHEDULE	
4. PERFORMING ORGANIZATION REPORT NUMBER(S) AFIT/GEO/ENP/88D-3	5. MONITORING ORGANIZATION REPORT NUMBER(S)
6a. NAME OF PERFORMING ORGANIZATION School of Engineering 6b. OFFICE SYMBOL (If applicable) AFIT/ENP	7a. NAME OF MONITORING ORGANIZATION
6c. ADDRESS (City, State, and ZIP Code) Air Force Institute of Technology Wright-Patterson AFB, OH 45433	7b. ADDRESS (City, State, and ZIP Code)
8a. NAME OF FUNDING / SPONSORING ORGANIZATION 8b. OFFICE SYMBOL (If applicable)	9. PROCUREMENT INSTRUMENT IDENTIFICATION NUMBER
8c. ADDRESS (City, State, and ZIP Code)	10. SOURCE OF FUNDING NUMBERS PROGRAM ELEMENT NO. / PROJECT NO. / TASK NO / WORK UNIT ACCESSION NO.

11. TITLE (Include Security Classification)
EVALUATION OF THE SPATIAL AND TEMPORAL CHARACTERISTICS OF THE CONDUCTING PRIZ (Unclas.)

12. PERSONAL AUTHOR(S)
Patrick J. Gardner, B.S., Captain, USAF

13a. TYPE OF REPORT	13b. TIME COVERED	14. DATE OF REPORT (Year, Month, Day)	15. PAGE COUNT
MS Thesis	FROM _____ TO _____	1988, December	50

16. SUPPLEMENTARY NOTATION

17. COSATI CODES			18. SUBJECT TERMS (Continue on reverse if necessary and identify by block number)
FIELD	GROUP	SUB-GROUP	PRIZ, Conducting PRIZ, BSO, Spatial Light Modulator, Dynamic Image Selection
20	06		

19. ABSTRACT (Continue on reverse if necessary and identify by block number)

Thesis Chairman: Dr. Theodore E. Luke

Approved for release in Accordance with AFR 190-1
[signature]
12 Jan 1989

The imaging properties of the conducting PRIZ were re-evaluated using crystals which were carefully ground and polished to minimize surface layer damage. Resolution was quantified as a function of the energy density of the write-beam for both incoherent and coherent light sources. Maximum resolution from a standardized bar chart was determined using a model derived from a hybrid of luminance ratios used to evaluate image quality and the Rayleigh criteria for two point resolution. In addition, the spatial-temporal frequency dependence of the conducting PRIZ in the dynamic imaging (Continued on reverse)

20. DISTRIBUTION / AVAILABILITY OF ABSTRACT	21. ABSTRACT SECURITY CLASSIFICATION
☒ UNCLASSIFIED/UNLIMITED ☐ SAME AS RPT. ☐ DTIC USERS	UNCLASSIFIED
22a. NAME OF RESPONSIBLE INDIVIDUAL Dr. Theodore E. Luke	22b. TELEPHONE (Include Area Code) 513-255-2012
	22c. OFFICE SYMBOL AFIT/ENP

DD Form 1473, JUN 86 *Previous editions are obsolete.* SECURITY CLASSIFICATION OF THIS PAGE

UNCLASSIFIED

(Continued from Block 19)

mode was demonstrated and, for the the first time, quantified for coherent illumination over a range of spatial and temporal frequencies. Finally, the write-beam- induced damage threshold for these carefully prepared crystals was determined in terms of energy density.

For an incoherent write-beam with light in the 360-510 nm range, the maximum measured resolution was found to peak at 20 lp/mm and 25 $\mu J/cm^2$. Coherent illumination with a HeCd laser at 442 nm produced peak resolution of 40 lp/mm at 90 $\mu J/cm^2$. Additional energy on the device did not improve the output resolution. Optical memory of the device was found to last for 20-60 minutes, depending on the specific spatial frequency, at these peak energy densities when a single pulse of write-beam was applied. When multiple pulses of write-beam energy were applied, the frequency of the pulses (temporal frequency) as well as the energy density of the beam and spatial frequency of the object influenced memory decay. These memory characteristics have direct implications on using the conducting PRIZ as a moving target indicator.

Catastrophic damage was found to occur for write-beam energy densities of 1150-1430 $\mu J/cm^2$ at low spatial frequencies and at higher energy densities for higher spatial frequencies. This is only slightly higher than that reported in previous AFIT research, although spatial frequency of an input image had not been previously considered a variable.

→ Keywords: Bismuth Silicon Oxide; Spatial light modulator